# *O detetor infravermelho da Cascavel*

Roland Köberle

Department of Physics/DipteraLab - USP-São Carlos, Brasil

Café com Física *São Carlos 2014*

Colaboradores:
Ifsc: J. Slaets, R. Pinto, L. Almeida, I. Zucoloto, R. Batista

Unesp Rio Claro: G. Gomes, D. Andrade; UFPe : P. Carelli.

Experimentos: Unesp Rio Claro

# O detetor infravermelho da Cascavel

Roland Köberle

IFSC-DipteraLab
Department of Physics/DipteraLab
USP-São Carlos, Brasil

September 18, 2014

Colaboradores:
Ifsc: J. Slaets, R. Pinto, L. Almeida, I. Zucoloto, R. Batista

Unesp Rio Claro: G. Gomes, D. Andrade; UFPe : P. Carelli.

# Typical pit organs

*Infrared Organs of Snakes: J. Herpetology, 45, No.1, 2011.*, R. C. Goris (2011)

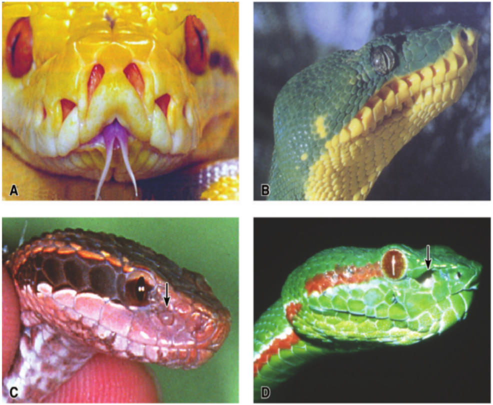


FIG. 1. Typical snakes possessing pit organs. (A) *Python molurus*, albino (Pythonidae). (B) *Corallus caninus* (Boidae). (C) *Gloydius blomhoffii* (Crotalinae, terrestrial). (D) *Trimeresurus stejnegeri* (Crotalinae, arboreal). The arrows in C and D point to the pit. Modified from Goris et al., 2010.

# Pit organ innervation



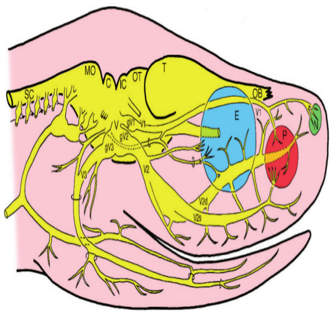


Fig. 3. Innervation of the crotaline pit organ. The pit membrane (red) is innervated by three branches of the trigeminal nerve (yellow). Abbreviations: C, cerebellum; E, eyeball (blue); IC, inferior colliculus; MO, medulla oblongata; N, nostril (green); OB, olfactory bulb; OT, optic tectum; P, pit; SC, spinal cord; V, trigeminal ganglion; V1, ophthalmic branch of the trigeminal (gv1, its ganglion); V2, maxillary branch of the trigeminal (gv2, its ganglion); V2d, deep branch of the maxillary branch; V2s, superficial branch of the maxillary branch; V3, mandibular branch of the trigeminal (gv3, its ganglion). The circles around V3 and other nerve trunks indicate the position of foramina in the cranial bones (not shown) where the nerve trunk enters or leaves the skull. Modified from Goris et al., 2010. Color reproduction supported by the Thomas Beauvais Fund.

Goris (2011)//

# Chegando ao Teto Optico

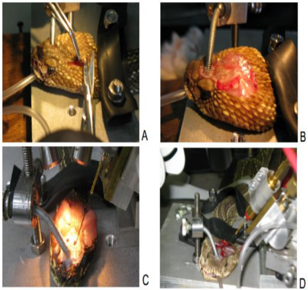


**Figura 15** - Passos da cirurgia efetuada na cascavel. A) Com a cobra entubada retira-se a pele do topo da cabeça. B) Fixa-se sua cabeça através de uma haste no osso entre os olhos (com resina de dentista). C) e D) Exposição do teto óptico, utilizando uma broca de dentista, com a retirada de uma parte do osso do crânio.

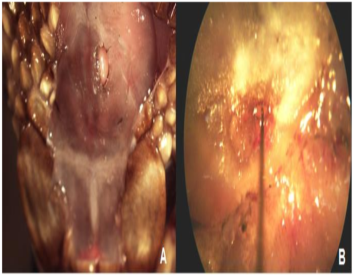


**Figura 16** - A) Teto óptico mostrando através da cabeça da cobra B) Teto óptico sendo mostrado através do microscópio; eletrodo penetrando nele.

Dissertação R. Batista

# Pit organ cross section

Goris (2011)

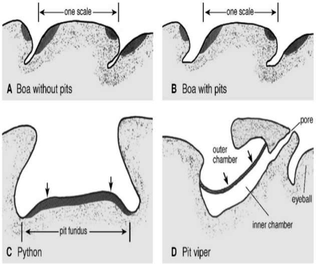


2. Diagrammatic cross-sectional morphology of snake infrared receptor organs. Hatching indicates the location of the receptor terminals. (A) d without pits (e.g., *Boa constrictor*). The receptors are located on the proximal and distal edges of the labial scales. (B) A boid with pits (e.g., *us caninus*). The receptors are found in essentially the same locations as in boids without pits, but the scales with receptors are separated by a invagination. (C) A pythonid (e.g., *Python molurus*). The receptors are located in the pit fundus, which acts as a retina, such that the anging mouth of the pit is able to act as the aperture of a pinhole camera. (D) A crotaline (e.g., *Gloydius blomhoffii*). The receptors are suspended from the body in a membrane that acts as a retina. The mouth of the pit is proportionately narrower than in the pythonids, acting as a better le aperture. Being suspended away from the body, the receptors have a lower heat capacity and, thus, greater sensitivity than those of the nids. The pore serves to equalize the atmospheric pressure on both sides of the membrane, as does the eustachian canal in the mammalian ear.

8 R. C. GO

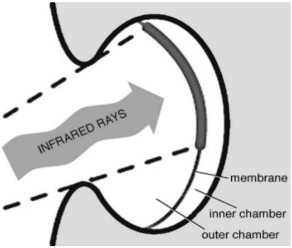


FIG. 7. The pinhole camera effect. An infrared source throws the shadow of the pit mouth onto the membrane receptors, exciting the receptors one after another as it moves, creating a unique series of action potentials, which the central nervous system interprets as a pattern. Modified from Goris et al., 2010.

Hartline 1982: Some 7000 thermosensitive

nerve endings of trigeminal sensory axons

on the 15 $\mu$ thick membrane with area 30 $\mu^2$.

TNM = Terminal Nerve Masses, Goris(2011)

# Estrutura superficial e direcional da membrana



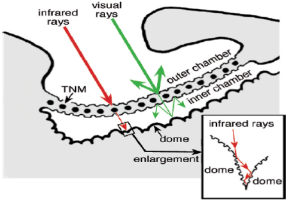


Fig. 9. Illustration of how the surface architecture of the pit organ shown in Figure 8 makes the organ selective for infrared radiation. The micropits of Figure 8B form an optical grating that passes the long wavelengths of infrared radiation (red lines), allowing them to stimulate the receptors (black dots) but reflecting away the shorter wavelengths of the visual spectrum (green lines). Some visual rays will pass through the translucent membrane, but these will be dispersed by the micropits on the surface of the domes from the inner chamber back wall (Fig. 8C) and, further, by the micropits on the inner surface of the pit membrane. Some infrared rays will also penetrate the membrane, but these will be absorbed in the light trap formed by the clustered large and small domes of Figure 8C and illustrated in the enlargement. Modified from Goris et al., 2010. Color reproduction supported by the Thomas Beauvais Fund.

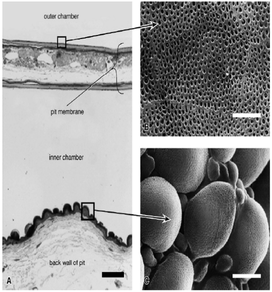


Fig. 8. Examples of the surface architecture of the pit organ of a pit viper, *Gloydius blomhoffii*. (A) Light micrograph of a cross-section through the pit. The bracket shows the pit membrane. Bar = 10 µm. (B) A scanning electron micrograph of the outer surface of the pit membrane at the point indicated by the upper box. Bar = 5 µm. (C) Scanning electron micrograph of the surface of the back wall at the point indicated by the lower box. Bar = 2.5 µm. Modified from Goris et al., 2010.

(Goris-2011)

Electron micrograph of single TNM

Pit Capillary System - Goris (2011)

RED RECEPTORS 5

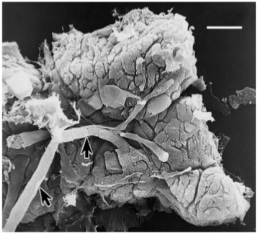

FIG. 4. A scanning electron micrograph of a single TNM viewed from the inner chamber. The pit membrane contains several thousands of these arrayed in a single layer just beneath the outer epidermis of the membrane. Lower arrow indicates the single myelinated nerve fiber that terminates in the TNM. Upper arrow shows the point where the nerve loses its myelin sheath and branches out to form the nerve mass. Bar = 10 μm. From Goris et al., 2010.


FIG. 10. The capillary bed of a pit membrane (*Gloydius blomhoffii*). The blood vessels have been visualized by perfusion with India ink. Each capillary loop encloses a finite number of TNMs. In actuality the membrane is concave; slits have been cut around the edges to make it lie flat. R, rostral; D, dorsal. Bar = 250 μm.

# Electron micrograph crossection of pit membrane (2010)

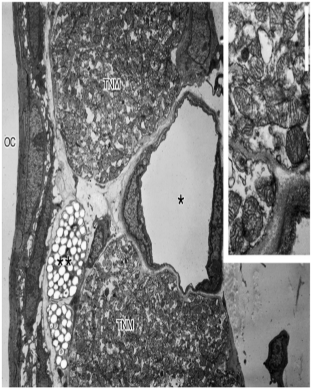


FIG. 13. A transmission electron micrograph of a cross-section through the pit membrane of a pit viper, *Gloydius blomhoffii*, showing how a capillary (asterisk) contacts two TNMs, presumably for cooling them. The inset shows a magnified view of the tightly packed mitochondria in a TNM. Abbreviations: *, capillary; **, organ of unknown function; OC, outer chamber. Bar = 4 μm. Modified from Goris et al., 2010.

Table 1
Properties of biological infrared imaging and sensing organs and thermoreceptors

| Animal/Insect | Threshold energy ($\mu W/cm^2$) | Threshold temperature change (°C) | Distance to detection | Type of receptor | Directional sensitivity | Reference |
|---|---|---|---|---|---|---|
| Boid IR receptor (*Boa constrictor*) | 176.89 | 0.003 | 16.4 cm | Specific warm | No | Barrett et al. (1970); de Cock Buning (1983); Molenaar (1992). |
| Boid pit organ (*Python reticulatus*) | 59.75 | 0.026 | 28.3 cm | Non-specific warm bimodal (IR and tactile) | Yes | Barrett et al. (1970); de Cock Buning (1983); Molenaar (1992) |
| Crotaline pit organ (*Agkistrodon rhodostoma*) | 10.75 | 0.003 | 66.3 cm | Specific warm | Yes | de Cock Buning (1983); Molenaar (1992) |
| Beetle antennal thermoreceptors (*Melanophila acuminata*) | May detect fires at short range | 2.0 | N/A | Warm receptor | Yes | Evans (1964) |
| Beetle pit organ (*Melanophila acuminata*) | 60–500 | 0.01 | 60–100 miles | Warm receptor | Yes | Schmitz and Bleckmann (1998) |
| Common vampire bat pit organs (*Desmodus rotundus*) | 50 | – | 8–12 cm | Warm receptor | Yes | Kurten and Schmidt. (1985); Molenaar (1992) |
| Blood-sucking insect antennae (*Itratoma infestans*) | – | Orient toward objects between 30 and 32°C | 4–10 cm | No receptor identified yet | Yes | Lazzari and Nunez (1989) |
| Butterfly wing vein thermoreceptors (*Troides r. plateni*) | – | Respond to heating rate of 2.4–4°C/s | N/A | type II receptors (warm) | Yes | Schmitz and Wasserthal (1993) |
| Butterfly antennal thermoreceptors (*Troides r. plateni*) | – | May measure ambient temperatures | N/A | Type I receptor (warm) | Yes | Schmitz and Wasserthal (1993) |

*A.L. Campbell et al. / Micron 33 (2002) 211–225*

# Recording from Optical Tectum

Goris et al. 2010

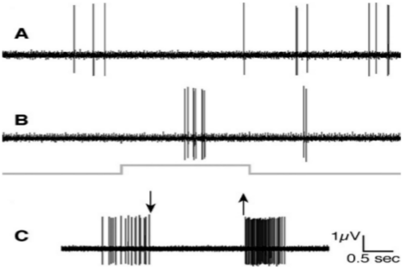


FIG. 5. Typical action potentials recorded from infrared neurons in snakes possessing infrared organs, in this case from the optic tectum of *Gloydius brevicaudus*. (A) Spontaneous discharge. Infrared neurons constantly produce action potentials at irregular intervals, caused by random stimulation by objects in the visual field of the pit all of which, by the laws of physics, emit infrared radiation of varying strength. (B) Stimulation by an infrared (830-nm) laser. The neuron responds with a burst of firing, with a varying degree of latency depending on the individual neuron. This is part of the encoding, which eventually produces a conscious image in the central nervous system. The solid line shows the onset, duration, and cessation of the laser. A and B are from the same neuron. (C) Response to a cold object (a popsicle). Arrows indicate the points at which the popsicle entered and left the pit's field of view. The spontaneous discharge at left ceases abruptly and responds with a strong burst when the stimulating object leaves the field of view. This shows that the infrared neuron can respond to an object whose temperature is lower than the background radiation, for example, a wet frog. The scale refers to all records. Modified from Goris

Hartline 1983 - IR and Visual Space

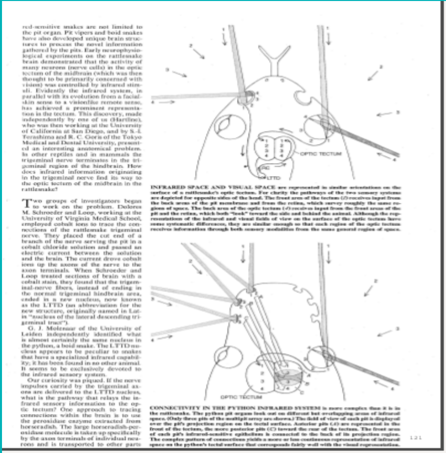

red-sensitive snakes are not limited to the pit organ. Pit vipers and boid snakes have also developed unique brain structures to process the novel information gathered by the pits. Early neurophysiological experiments on the rattlesnake brain demonstrated that the activity of many neurons (nerve cells) in the optic tectum of the midbrain (which was then thought to be primarily concerned with vision) was controlled by infrared stimuli. Evidently the infrared system, in parallel with its evolution from a facial-skin sense to a visionlike remote sense, has achieved a prominent representation in the tectum. This discovery, made independently by one of us (Hartline), who was then working at the University of California at San Diego, and by S.-I. Terashima and R. C. Goris of the Tokyo Medical and Dental University, presented an interesting anatomical problem. In other reptiles and in mammals the trigeminal nerve terminates in the trigeminal region of the hindbrain. How does infrared information originating in the trigeminal nerve find its way to the optic tectum of the midbrain in the rattlesnake?

Two groups of investigators began to work on the problem. Dolores M. Schroeder and Loop, working at the University of Virginia Medical School, employed cobalt ions to trace the connections of the rattlesnake trigeminal nerve. They placed the cut end of a branch of the nerve serving the pit in a cobalt chloride solution and passed an electric current between the solution and the brain. The current drove cobalt ions up the axons of the nerve to the axon terminals. When Schroeder and Loop treated sections of brain with a cobalt stain, they found that the trigeminal-nerve fibers, instead of ending in the normal trigeminal hindbrain area, ended in a new nucleus, now known as the LTTD (an abbreviation for the new structure, originally named in Latin "nucleus of the lateral descending trigeminal tract").

G. J. Molenaar of the University of Leiden independently identified what is almost certainly the same nucleus in the python, a boid snake. The LTTD nucleus appears to be peculiar to snakes that have a specialized infrared capability; it has been found in no other animal. It seems to be exclusively devoted to the infrared sensory system.

Our curiosity was piqued. If the nerve impulses carried by the trigeminal axons are delivered to the LTTD nucleus, what is the pathway that relays the infrared sensory information to the optic tectum? One approach to tracing connections within the brain is to use the peroxidase enzyme extracted from horseradish. The large horseradish-peroxidase molecule is taken up specifically by the axon terminals of individual neurons and is transported to other parts



INFRARED SPACE AND VISUAL SPACE are represented in similar orientations on the surface of a rattlesnake's optic tectum. For clarity the pathways of the two sensory systems are depicted for opposite sides of the head. The front area of the tectum (1) receives input from the back areas of the pit membrane and from the retina, which survey roughly the same regions of space. The back area of the optic tectum (4) receives input from the front areas of the pit and the retina, which both "look" toward the side and behind the animal. Although the representations of the infrared and visual fields of view on the surface of the optic tectum have some systematic differences, they are similar enough so that each region of the optic tectum receives information through both sensory modalities from the same general region of space.



CONNECTIVITY IN THE PYTHON INFRARED SYSTEM is more complex than it is in the rattlesnake. The python pit organs look out on different but overlapping areas of infrared space. (Only three pits of the multipit array are shown.) The field of view of each pit is displayed over the pit's projection region on the tectal surface. Anterior pits (A) are represented in the front of the tectum, the more posterior pits (C) toward the rear of the tectum. The front area of each pit's infrared-sensitive epithelium is connected to the back of its projection region. The complex pattern of connections yields a more or less continuous representation of infrared space on the python's tectal surface that corresponds fairly well with the visual representation.

121

Directional Sensitivity - Bakken 2012

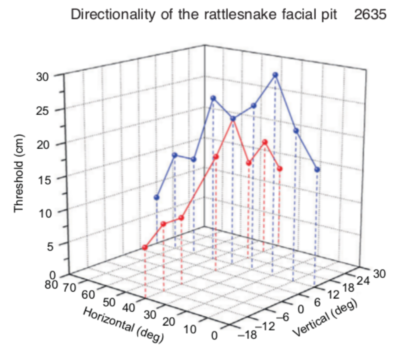


Fig. 8. Plot of directional sensitivity of the facial pit of *C. atrox*. Along both the horizontal (blue) and vertical (red) transects the facial pit exhibits clear directional sensitivity. Threshold ($z$-axis) represents the greatest distance (up to a maximum of 30 cm) between emitter and facial pit that generated a significant neural response of background activity.

Water flowing onTrigeminal Nerve - Bullock 1956, $\Delta T \sim 0.025^{\circ}C$

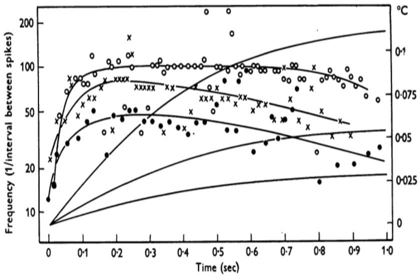


Text-fig. 4. Sensitivity measured by change in temperature. Water flowing at constant rate over the pit membrane is electrically heated from a certain moment. Three different rates of temperature rise, estimated by reading thermocouple records at 0·3, 1·0 and 2·0 sec. Response measured as interval between successive spikes except at high frequency, when the average interval for two or three successive spikes is plotted. The upper, middle and lower hand drawn curves (circles, crosses and dots, respectively) correspond to the stimulus curves in the same relative positions. There is uncertainty in the position of zero time on the record, owing to the small thermocouple deflexion, of about 0·1 sec. Nevertheless, the response is very abrupt and permits estimation of the $\Delta T$ approaching threshold. Ordinate at right in °C.

Bakken & Krochmal(2007). Thus, the membrane may conceivably respond to contrasts of less than $0.001^{\circ}$C (Recording response threshold from Trigeminal Nerve). The mechanism by which such sensitivity might be obtained is presently unknown.

# Pit:

1. innervated by two ganglia of the trigeminal nerve.
   Warm myelinated A-delta fibers from the Ophthalmic ganglion: innervate dorsal part of membrane, Maxillary ganglion: two bundles innervate the ventral and rostral areas of the membrane.
   Terminals of nerves from these ganglia innervate unevenly the pit membrane ($\sim 600$ fibres),but each has its own *territory* within the membrane.
2. Pit membrane is also innervated by scores of unmyelinated C fibers, some of which are probably nociceptive fibers, whereas others may belong to the autonomic (sympathetic and parasympathetic) nerve system controlling the blood vessels of the membrane.
3. Sensory receptors of all kinds contain a more-or-less large number of mitochondria, but the mitochondria in the snake TNMs surpass by far the numbers in other known sensory organs. It may be that these massed mitochondria form part of the mechanism, whereby the pit receptors respond extremely rapidly to minute temperature changes, but this has yet to be proven.

(Goris 2011, Goris and Nomoto, 1967; Goris and Terashima, 1973; Kishida et al., 1980; Berson and Hartline, 1988).

# Molecular structure

*Gracheva et al.: Molecular basis of the infrared detection by snakes. Nature 464:1006-1012, 2010.*

Pit membrane:

Passive antenna for radiant heat,
transducing thermal energy to heat-sensitive channels on embedded nerve fibres.
→ Snake TRPA1 is a heat-activated channel.

TRPA1 roperties:

- inactive at room temperature,
- but robustly activated above $27.6 \pm 0.9^\circ$C.
- no response to cold ($12^\circ$C).

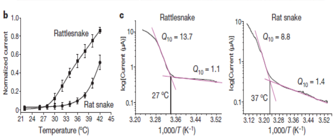


**Figure 3 | Functional analysis of snake TRPA1 channels.** **a**, HEK293 cells expressing cloned rattlesnake or rat snake TRPA1 channels were analysed for heat or mustard oil (200 μM AITC; 24 °C)-evoked responses using calcium imaging; colour bar indicates relative change in fluorescence ratio, with purple and white denoting the lowest and highest cytoplasmic calcium, respectively ($n \geq 105$ cells per channel). **b**, Relative heat response profiles of rattlesnake and rat snake channels expressed in oocytes (response at each temperature was normalized to the maximal response at 45 °C; holding potential ($V_H$) = −80 mV; $n \geq 6$). Data show mean ± s.d. **c**, Arrhenius plots show thermal thresholds and $Q_{10}$ values for baseline and evoked responses of rattlesnake (left) and rat snake (right) TRPA1 channels, as indicated (temperature ramp of 1 °C s$^{-1}$).

Threshold much too high to explain our data!

# Firing Patterns

The firing patterns of neurons associated with pits at all levels of the nervous system (peripheral nerves, medulla oblongata, optic tectum, nucleus rotundus of the thalamus, anterior dorsal ventricular ridge of the telencephalon; for details, see below) have three common characteristics.
(Goris 2011, Goris and Nomoto, 1967; Goris and Terashima, 1973; Kishida et al., 1980; Berson and Hartline, 1988).

1. The neurons of other sensory modes (e.g., lateral eye vision) are silent. In contrast, infrared neurons fire constantly at irregular intervals. All objects,constantly give off infrared radiation generating *spontaneous discharge*. At a body temperature of $25^{\circ}$C, frequency is 10-30 spikes/sec (varies with species, body temperature, and individual neurons).
2. Firing increases in response to any stimulus of higher temperature (or stronger IR radiation ) than the background. Firing frequency changes with IR $\lambda$ of the stimulus, strongest at

   $$\lambda = 3 - 15\mu m$$

   = wavelength normally radiated from the body surface of endothermic animals
3. For temperature lower than that of the background → firing frequency decreases (e.g., Bullock and Diecke, 1956; Goris and Nomoto,1967; Fig. 5C).

# Um pouco de Física

## Radiação do Corpo Negro.

**Radiation by unit volume and unit solid angle**

$1\ cal = 4.1868\ W sec$ $\qquad k = 1.381 \cdot 10^{-23}\ J/^{\circ} K$

$c = 3 \cdot 10^{8}\ m/sec$ $\qquad \hbar = 6.600 \cdot 10^{-34}\ J \cdot s$

$T_0 = 273.16^{\circ} K$ $\qquad \sigma = 5.6522 \cdot 10^{-8} \frac{W}{m^2 \cdot K^4}.$

Spectral densitiy $[E/V/d\Omega]$ is

$$e_0(\omega) = \frac{1}{V} \frac{2 \cdot 4\pi}{(2\pi)^3} \frac{dE_\omega}{d\omega} = \frac{\hbar\omega^3}{4\pi^3 c^3 (e^{\hbar\omega/kT} - 1)}$$

## Radiation by hemisphere

Emitted flux by surface $\hat{n}$:

. $J(\omega,\theta)\ d\Omega = ce_0(\omega) d\Omega = ce_0(\omega)$

Emitted flux falling on unit surface S tilted by $\hat{n}\cdot\hat{n}_S = \cos\theta$:

. $J(\omega,\theta)\cos\theta d\Omega$

Total emitted flux falling on S:

. $J_0 = c\int_0^\infty e_0(\omega) d\omega$

Integration over frequencies yields

. $\int_0^\infty e_0(\omega) d\omega = \int_0^\infty \frac{\hbar\omega^3 d\omega}{4\pi^3 c^2 (e^{\hbar\omega/kT} - 1)} = \frac{\hbar}{4\pi^3 c^2}(\frac{kT}{\hbar})^4 \int_0^\infty \frac{x^3 dx}{e^x - 1)} = \frac{(kT)^4}{4\pi^3 c^2 \hbar^3}\frac{\pi^4}{15}$,

Including the solid angle integration: get total flux $W/m^2$

$$J_0 = \frac{(kT)^4}{4\pi^3 c^2 \hbar^3}\frac{\pi^4}{15} \qquad = \sigma T^4 \text{ (Stefan-Boltzmann)}$$

with $\sigma = \frac{\pi^2 k^4}{60\hbar^3 c^2}$.

For conical radiative aperture with angle $\theta$, instead of emitting half-sphere: $J_0(\theta) = \sigma T^4 \sin^2\theta$.

# Energy Flux: experimental results

Previous Experimental Results from nerve recordings

1. Bullock(1956):
   Trigeminal nerve recording and supposing all IR radiation is absorbed:
   Threshold flux $\Delta\Phi = 75\ \mu W/cm^2$;

   Single fiber recording with water flowing on pit membrane:
   $\Delta T_{min} \sim 0.003^\circ C$
   *These figures cannot be given great reliability because this sensitivity pushes to the limit the usefulness of the available temperature recording system and we are not sure of the form of the initial change in temperature.*
2. Goris et al.(1967):
   IR-laser
   $\Delta\Phi \sim 100\ \mu W/cm^2$ at membrane.

Experimental Results using $\simeq \sigma(T_1^4 - T_2^4)(R/D)^2$

1. Buning et al.(1981):
   Shutter-Signal *independent* of background, record from midbrain tectum
   $\Delta\Phi = 10.76\ \mu W/cm^2$.
2. Ebert & Westhoff (2006):
   Shutter, Behavioral threshold for Crotalus atrox:
   $\Delta\Phi = 3.35\ \mu W/cm^2$
   for $D = 100\ cm$.

**Figura 24** - Experimento sendo realizado com o braço mecânico e placa peltier.

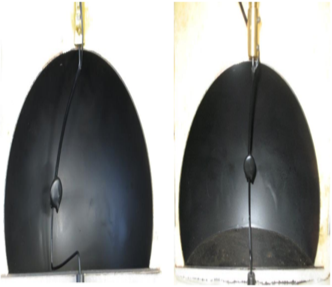

**Figura 22** - Foto do estímulo. Resistência circular acoplada no meio de arco de alumínio, dentro da cúpula de cobre (Todos devidamente pintados com tinta fosca preta).

Rio Claro, Dissertação R. Batista

# Rio Claro results for $\Delta T$

For a response threshold of $\sim 3^\circ C$, we get

All wavelength: $\Delta T_{Min} \sim 0.01^\circ C$.

Assuming absorption only in the $\lambda = 4 - 15 \mu m$: $\Delta T_{min} \sim 0.005^\circ C$!

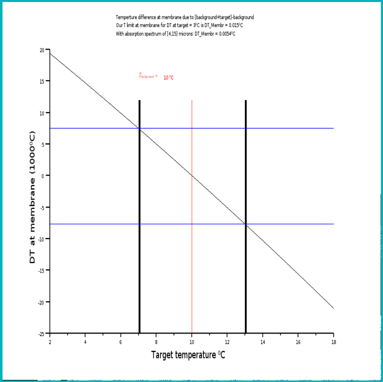

## Numbers for our Experimental Setup

Total radiative heat flux is $\sim$ time-independent!

For

IR background temperature $T_f$ =10$^\circ C$, Moving target radiating area $A_a = 2 * 2\ cm^2$,

Moving target temparture $T_a =$ 13$^\circ C$ , Backgound radiating area $A_f = 10 * 10 cm^2$

Target to Pit distance $D = 10\ cm$, $f_\lambda \sim 1/2$

The fluxes are:

$$\Phi_f \quad = \left(\frac{\sigma}{4\pi D^2}\left[T_f^4 A_f\right]\right) f_\lambda \qquad = \quad 2359.78\ \frac{\mu W}{cm^2},$$

$$\Phi_{f+a} = \left(\frac{\sigma}{4\pi D^2}\left[T_f^4 (A_f - A_a) + T_a^4 A_a\right]\right) f_\lambda = \quad 2368.93\ \frac{\mu W}{cm^2}$$

For IR-wavelenghts the irradiance contrasts are:

$$\delta\Phi = \Phi_{f+a} - \Phi_f = \frac{\sigma}{4\pi D^2}(T_a^4 - T_f^4) A_a f_\lambda = 9\ \frac{\mu W}{cm^2}.$$

## Signal to Pit-background ratio:

- Signal Flux: $\delta\Phi = 9 \; \frac{\mu W}{cm^2}$.
- Heat flux from snake's pit: $T_{pit} = 22^\circ C$, $\epsilon_{pit} = 0.3$
  $\Phi_{pit} = \sigma T_{pit}^4 \epsilon_{pit} f_\lambda = 6650 \; \frac{\mu W}{cm^2}$.
- Include membrane absoprtion factor: $\epsilon_{abs} \sim 0.5 \rightarrow$

$$S = (\epsilon_{abs}\Phi_{pit})/\delta\Phi \sim 350$$

- Temos um problema aqui ????

## Signal to Pit-background ratio:

- Signal Flux: $\delta\Phi = 9\ \frac{\mu W}{cm^2}$.
- Heat flux from snake's pit: $\Phi_{pit} = \sigma T_{pit}^4 \epsilon_{pit} f_\lambda = 6650\ \frac{\mu W}{cm^2}$.

$T_{pit} = 22^\circ C$, $\epsilon_{pit} = 0.3$

- Include membrane absoprtion factor: $\epsilon_{abs} \sim 0.5 \to$

$$S = (\epsilon_{abs}\Phi_{pit})/\delta\Phi \sim 350$$

- Temos um problema aqui ????

## Signal to Pit-background ratio:

- Signal Flux: $\delta\Phi = 9\ \frac{\mu W}{cm^2}$.
- Heat flux from snake's pit: $T_{pit} = 22^\circ C$, $\epsilon_{pit} = 0.3$

  $\Phi_{pit} = \sigma T_{pit}^4 \epsilon_{pit} f_\lambda = 6650\ \frac{\mu W}{cm^2}$.

- Include membrane absoprtion factor: $\epsilon_{abs} \sim 0.5 \rightarrow$

$$S = (\epsilon_{abs}\Phi_{pit})/\delta\Phi \sim 350$$

- Temos um problema aqui ????

## Signal to Pit-background ratio:

- Signal Flux: $\delta\Phi = 9\ \frac{\mu W}{cm^2}$.
- Heat flux from snake's pit: $T_{pit} = 22^\circ C$, $\epsilon_{pit} = 0.3$
  $\Phi_{pit} = \sigma T_{pit}^4 \epsilon_{pit} f_\lambda = 6650\ \frac{\mu W}{cm^2}$.
- Include membrane absoprtion factor: $\epsilon_{abs} \sim 0.5 \rightarrow$

$$S = (\epsilon_{abs}\Phi_{pit})/\delta\Phi \sim 350$$

- Temos um problema aqui ????

*Modelling a Historic Oil-Tank Fire Allows an Estimation of the Sensitivity of the Infrared Receptors in Pyrophilous Melanophila Beetles*, Helmut Schmitz, Herbert Bousack (2012)

Beetles coming from 60 − 130 km!

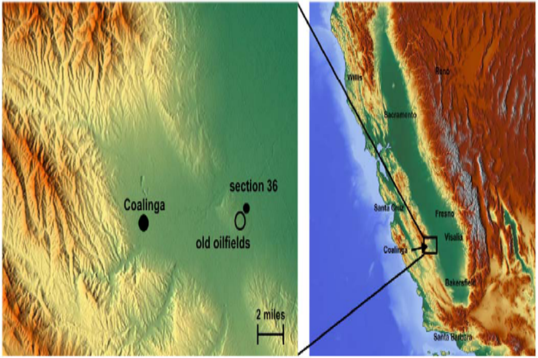


**Figure 2. Identification of section 36 and the place of the old oilfields using [24,98].**
doi:10.1371/journal.pone.0037627.g002

# IR detector from *first* principles.

- Problem: detect infra-red radiation embedded in infra-red background.
  Nobody tells how heat accumulated in membrane is carried off! In the vicinity ($\sim 200\mu m$) of laser stimulation ($\lambda = 0.8\mu m$) get $50$ % increase in blood flow in $\sim 4.5$ msec! (Goris 2007)
- Equivalent problem in Vision:
  Detect a light source embedded in an environment at temperature

$$T_{equivalent} = \frac{\lambda_{infrared}}{\lambda_{visible}} = 10000^{\circ} K$$

- The whole Pit Organ would blaze like the sun!
- Is mechanical deformation of the pit an effective stimulus?

# IR detector from *first* principles.

- Problem: detect infra-red radiation embedded in infra-red background.
  Nobody tells how heat accumulated in membrane is carried off! In the vicinity ($\sim 200\mu m$) of laser stimulation ($\lambda = 0.8\mu m$) get $50$ % increase in blood flow in $\sim 4.5$ msec! (Goris 2007)
- Equivalent problem in Vision:
  Detect a light source embedded in an environment at temperature

$$T_{equivalent} \equiv \frac{\lambda_{infrared}}{\lambda_{visible}} = 10000^{\circ} K$$

- The whole Pit Organ would blaze like the sun!
- Is mechanical deformation of the pit an effective stimulus?

# IR detector from *first* principles.

- Problem: detect infra-red radiation embedded in infra-red background.
  Nobody tells how heat accumulated in membrane is carried off! In the vicinity ($\sim 200\mu m$) of laser stimulation ($\lambda = 0.8\mu m$) get $50$ % increase in blood flow in $\sim 4.5$ msec! (Goris 2007)
- Equivalent problem in Vision:
  Detect a light source embedded in an environment at temperature

$$T_{equivalent} \equiv \frac{\lambda_{infrared}}{\lambda_{visible}} = 10000^{\circ} K$$

- The whole Pit Organ would blaze like the sun!
- Is mechanical deformation of the pit an effective stimulus?

# IR detector from *first* principles.

- Problem: detect infra-red radiation embedded in infra-red background.
  Nobody tells how heat accumulated in membrane is carried off! In the vicinity ($\sim 200\mu m$) of laser stimulation ($\lambda = 0.8\mu m$) get $50$ % increase in blood flow in $\sim 4.5$ msec! (Goris 2007)
- Equivalent problem in Vision:
  Detect a light source embedded in an environment at temperature
  $$T_{equivalent} \equiv \frac{\lambda_{infrared}}{\lambda_{visible}} = 10000^\circ K$$
- The whole Pit Organ would blaze like the sun!
- Is mechanical deformation of the pit an effective stimulus?

# Heating time/temperature dependence

Signal Flux $\delta\Phi = 9\ \frac{\mu W}{cm^2}$.

Energy increase due to signal on membrane

$\delta Q_{mbr} = \delta\Phi A_{mbr} = 1.15\ \mu W$.

*Membrane absorption factor* $\epsilon_{mbr} = 0.6$

$\delta Q_{mbr} = (\epsilon_{mbr} c_v V_{mbr} \rho_{mbr}) \delta T_{mbr}$ - data as for $H_2O$

Temperature change:

$\delta T_{mbr} = 0.002$ C°/sec

Is there enough machinery to carry off the heat???

$Q_{pit}/\delta Q_{mbr} = 1090$

What is the response-time of the membrane?

$\sim 4$ msec (Goris 2007)!

# Where do we stand?

**To do:**

1. Study dependence on target movement & contrast sharpness.
2. Include geometrical factors and positional dependence of $\epsilon_{abs}$.
3. a Provide an ideal IR-detector in the presence of background and noise.

   In contrast to statements by Bullock/Diecke (1956) and T. de Cock Buning (1983) arguing the independence on snake temparature!
4. Show that the detctor is compatible with pit anatomy & physiology.
5. What is the thermo-transduction mechanism?

# Where do we stand?

## To do:

1. Study dependence on target movement & contrast sharpness.
2. Include geometrical factors and positional dependence of $\epsilon_{abs}$.
3. a Provide an ideal IR-detector in the presence of background and noise.

   In contrast to statements by Bullock/Diecke (1956) and T. de Cock Buning (1983) arguing the independence on snake temparature!
4. Show that the detctor is compatible with pit anatomy & physiology.
5. What is the thermo-transduction mechanism?

# Where do we stand?

## To do:

1. Study dependence on target movement & contrast sharpness.
2. Include geometrical factors and positional dependence of $\epsilon_{abs}$.
3. a Provide an ideal IR-detector in the presence of background and noise.

   In contrast to statements by Bullock/Diecke (1956) and T. de Cock Buning (1983) arguing the independence on snake temparature!
4. Show that the detctor is compatible with pit anatomy & physiology.
5. What is the thermo-transduction mechanism?

# Where do we stand?

## To do:

1. Study dependence on target movement & contrast sharpness.
2. Include geometrical factors and positional dependence of $\epsilon_{abs}$.
3. a Provide an ideal IR-detector in the presence of background and noise.

   In contrast to statements by Bullock/Diecke (1956) and T. de Cock Buning (1983) arguing the independence on snake temparature!
4. Show that the detctor is compatible with pit anatomy & physiology.
5. What is the thermo-transduction mechanism?

# Where do we stand?

## To do:

1. Study dependence on target movement & contrast sharpness.
2. Include geometrical factors and positional dependence of $\epsilon_{abs}$.
3. a Provide an ideal IR-detector in the presence of background and noise.

   In contrast to statements by Bullock/Diecke (1956) and T. de Cock Buning (1983) arguing the independence on snake temparature!
4. Show that the detctor is compatible with pit anatomy & physiology.
5. What is the thermo-transduction mechanism?

# Effect of Snake Temperture - does it really cancel out?

Buning (1983)
Considers background irradiation by snake's body
Did experiment at ambient temperatures:
$21C^{\circ}$and $15C^{\circ}\rightarrow$ same threshold for response.

with and without chopper:
$\rightarrow$ snake-temperature cancels out in the difference.
*(Assumes instantaneous reaction to changes in temparture gradient.*
*Also: noise adds up!)*

# O que pode ajudar?

- Surface architecture
- *Discovery of a Novel Accessory Structure of the Pitviper Infrared Receptor Organ (Plos1 2013)*,
  Carlos Jared et al., Departamento de Zoologia, Instituto de Biociencias, USP
- Include heat lost/absorbed from membrane to air by convection
  Amount of heat lost by conduction through the air to the pit walls:
  Assume the snake being able to cool the membrane by

$$\delta T_{pit-mbr} = -0.1°\text{C}$$

Thermal conductivty of air: $k_{air} = \rho v c_p l_{mfp}/3 = 0.026 W m^{-1}/°C$ , Typical distances$\sim 1\, mm$

$$Q_{Air} = [k_{air}(1/d_1 + 1/d_2)] * \delta T_{pit-mbr} A_{mbr} = 65.345127\ \mu W$$

! Bakken & Krochmal 2007

# Shutter Experiment - Snake Temperature cancels

Originally this formula was designed to describe the net flux of radiation between two heat radiating objects with temperatures $T1$ and $T2$. Therefore, one tends to substitute for $T1$ the temperature of the pit organ (or the snake) and for $T2$ the temperature of the warm test object (or mouse/rat). However, in terms of physics the test situation described in this paper implies a change of radiant flux between before and after opening the shutter. Consequently, in the final formula the temperature of the snake is cancelled.

radiation density (cal/cm$^2 \cdot$ s) =

$$\frac{\sigma \times A}{\pi \times D^2} ((\mathrm{T}^4 \text{ stimulus} - \mathrm{T}^4 \text{ snake})$$

$$- (\mathrm{T}^4 \text{ shutter} - \mathrm{T}^4 \text{ snake})) =$$

$$\frac{\sigma \times A}{\pi \times D^2} (\mathrm{T}^4 \text{ stimulus} - \mathrm{T}^4 \text{ shutter}).$$

In other words, the change of radiant heat influx on the pit organs can be regarded as the result of a change in the infrared environment, i.e., that small area which only changes in temperature (in this case the shutter and heat exchanger or the presence or absence of a mouse).

This implicates that the temperature of the sensor is not relevant for the ability of the system to discriminate temperature differences in the environment. Although, the intensity of the receptor response towards a specific stimulus is, of course, a function of a biologically related optimum temperature of the body (de Cock Buning 1981 b, c; Hensel 1975), on the other hand, there is no argument from the physics to expect a relation between the threshold value and the temperature of the body. The same conclusion was reached by Bullock and Diecke (1956) and illustrated by one of their experiments. 'Experimentally, in a certain whole nerve preparation the response to a hand at 20 cm in a room equilibrated to 21 °C was about threshold. Wheeling the preparation and equipment into a cold room at 15 °C nearly doubled this distance, to 37 cm. There was no noticeable difference in threshold between the first moments when the snake's body temperature was still warm and spon-

# Protein dynamics of vibrational states

252 Proteins: Energy, Heat and Signal Flow

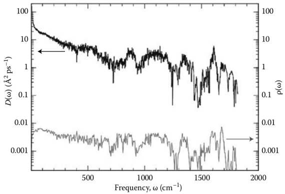


**FIGURE 11.1** Mode diffusivity (black) and vibrational mode density (gray) computed for myoglobin. At low frequency, to about 100–150 cm$^{-1}$, where the vibrational modes are delocalized, the mode diffusivity is relatively large and becomes smaller with increasing frequency, in contrast to the vibrational mode density. Trends in the two quantities parallel one another at higher frequency, where the vibrational modes are localized.

Yamato(1998)

Photoreaction: in general, however, the functionally important motion of a protein along the reaction coordinate is largely masked by the thermal fluctuatios, making it difficult to analyze the effect of an external stimulus on the protein dynamics (*Heat Transport in Proteins*, Leitner 2010).

# É isso ai pessoal!

Obrigado!